ELSEVIER

Thermochimica Acta 255 (1995) 155–170

thermochimica acta

Preparation and thermal dehydration of manganese(II) dicarboxylate hydrates

Yukihiko Suzuki

Department of Applied Chemistry, Faculty of Engineering, Yamagata University, Jonan, Yanezawa 992, Japan

Received 25 July 1994; accepted 1 October 1994

Abstract

Manganese(II) dicarboxylate hydrates $Mn[OOC(CH_2)_nCOO] \cdot xH_2O$ have been prepared by the addition of $MnCO_3$ powder or concentrated $MnSO_4$ solution to aqueous solutions of the corresponding dicarboxylic acids.

The crystal forms of the precipitated compounds were observed by optical microscopy. The crystals were obtained either as ellipsoidal, short rods or very small uneven particles. The crystals were different from those of the dicarboxylic acids. The dicarboxylates obtained were characterized by X-ray diffraction analysis and IR spectral measurement.

The thermal dehydrations of the Mn(II) dicarboxylate hydrates were investigated by TG–DTA. The temperatures at which dehydration occurred were taken as a measure of the strength of the $Mn-OH_2$ bond, and these were found to vary with increasing number of CH_2 groups in the dicarboxylic acid.

The kinetic parameters for the dehydration were calculated by employing a computation method. The three-dimensional diffusion model is found to be the best for describing the kinetic results for the main reaction.

Keywords: Coupled technique; Dehydration; DTA; Kinetics; Manganese dicarboxylate hydrate; TG

1. Introduction

An investigation into the characterization of metal dicarboxylates with both organic and inorganic properties is of great interest because these compounds

SSDI 0040-6031(94)02132-5

consist of carboxyl groups and metals. Although many investigations of the thermal decomposition reactions of metal dicarboxylates have been carried out [1], they have usually been investigated in isolation, e.g. the decomposition of oxalates and malonates [2], some succinates [3] and fumarates [4].

The effects of systematically varying the cations and keeping the same dicarboxylic anion on the thermal behaviour have been extensively investigated using TG and DTA [2]. There is, however, little or no literature on the thermal behaviour of a series of metal dicarboxylates with the same cation. Manganese(II) ions are labile, can occur in different valence states and will readily change from one valency to another in an air atmosphere. Manganese is fairly electro-positive, and Mn(II) ions form many complexes in which the metal ion is usually octaherdrally coordinated.

Most of these complexes contain no ligand field stabilization energy. The present paper reports the preparation, characterization and dehydration reactions of a series of Mn(II) dicarboxylates using optical microscopy, IR absorption spectrometry, X-ray powder diffractometry, TG and DTA.

2. Experimental

2.1. Purification of dicarboxylic acids

All the carboxylic acids starting materials used were purified by recrystallization from aqueous solutions of reagent grade dicarboxylic acids [$HOOC(CH_2)_nCOOH$]. The crystals obtained were filtered, washed with a mixed solution of ethanol and ether (2:1), and dried over P_2O_5 and then silica gel in a desiccator for several days.

The assay of the acid crystals was determined by titration with standard base.

2.2. Preparation of manganese(II) dicarboxylate hydrates

Mn(II) compounds were prepared by two different procedures.

(1) Oxalate, malonate, azelate, and sebacate were precipitated on reacting $MnCO_3$ powder with an aqueous solution of the corresponding dicarboxylic acids, in 10% excess, at 70°C.

(2) Succinate, glutarate, adipate, pimerate and suberate were obtained by the addition of the corresponding dicarboxylic acid solution to a solution of $MnSO_4$, adjusted to pH 7 with dilute NaOH solution.

In both cases, precipitation of the Mn(II) dicarboxylates occurred immediately. The solution was allowed to stand overnight at room temperature, the crystals were filtered, washed with water and a 2:1 mixture of ethanol and ether, dried by pressing gently between filter papers (Toyo Roshi No. 4), and stored over silica gel in a desiccator. The compounds obtained were pale pink crystalline powders.

Elemental analyses for C, H and Mn are given in Table 1. The number of water molecules depends entirely on the nature of the complex structure and also on the drying procedure [5]. The water of crystallization of the compounds was confirmed

Table 1
Analytical data for Mn(II) dicarboxylate hydrates

Compound	Formula	C/%		H/%		Mn/%	
		Found	Calcd.	Found	Calcd.	Found	Calcd.
Oxalate	$MnC_2O_4 \cdot 2H_2O$	13.45	13.42	2.24	2.25	30.33	30.70
Malonate	$MnC_3H_2O_4 \cdot 2H_2O$	18.72	18.67	3.09	3.13	28.04	28.46
Succinate	$MnC_4H_4O_4 \cdot 4H_2O$	18.52	19.76	4.27	4.98	21.83	22.60
Glutarate	$MnC_5H_6O_4 \cdot 4H_2O$	23.31	23.36	5.47	5.49	21.32	21.37
Adipate	$MnC_6H_8O_4 \cdot H_2O$	33.15	33.20	4.52	4.64	25.28	25.31
Pimelate	$MnC_7H_{10}O_4 \cdot H_2O$	35.85	36.38	5.02	5.23	23.48	23.77
Suberate	$MnC_8H_{12}O_4 \cdot H_2O$	39.42	39.20	5.42	5.76	22.40	22.41
Azelate	$MnC_9H_{14}O_4 \cdot H_2O$	42.75	41.71	6.16	6.22	21.91	21.20
Sebacate	$MnC_{10}H_{16}O_4 \cdot H_2O$	44.03	43.97	6.58	6.64	20.02	20.11

by elemental and TG analyses. The manganese contents in the dicarboxylates were determined by complexometric titrations with standard EDTA solutions using BT indicator.

2.3. Measurements

TG and DTA curves were obtained using a Seiko Denshi TG/DTA 30 differential microbalance at a heating rate of 10°C min^{-1} in flowing atmospheres of Ar, CO_2 and air at 200 ml min^{-1}.

About 30 mg of powder sample, in a platinum pan (7 mm in diameter, 70 μl in volume), was used in each experiment. X-ray powder diffraction analysis and IR spectral measurements were carried out as described in a previous paper [6].

2.4. Kinetic treatment

If the kinetic analysis is carried out with a TG curve obtained at a constant heating rate, $\phi = dT/dt$, and taking into account the Arrhenius equation, the expression

$$g(\alpha) = kt \tag{1}$$

becomes

$$g(\alpha) = \int_0^t k \, dt = \frac{AE_a}{\phi R} P(x) \tag{2}$$

where $x = E_a/RT$ and $g(\alpha)$ is a function depending on the actual kinetic law. It is based on the quick convergence of the $P(x)$ function, and Eq. (2), after taking logarithms and regrouping terms, can be written as

$$\log \frac{g(\alpha)}{T^2} = \log \frac{AE_a}{\phi R} - \frac{E_a}{2.3RT} \tag{3}$$

All data were transferred to an NEC 9800 VM microcomputer and linear plots were drawn for the general solid state rate forms [7] of log $g(\alpha)/T^2$ vs. $1/T$ by the least-squares method. E_a, A and the corresponding correlation coefficients (γ) for the linear plots were calculated. The high values of the coefficients show a good linearity, and the method which has the best linear relationship, i.e. the coefficient closest to unity, was selected.

3. Results and discussion

3.1. Crystal forms

Typical optical micrographs of the crystals prepared are shown in Fig. 1(a)–(d). The small, uneven crystal forms differed from those of the dicarboxylic acids which have been described in a previous paper [6]. The forms varied with the size of the carboxylic acid group: cubic for oxalate ($n = 0$), rods for malonate ($n = 1$), ellipsoids for succinate ($n = 2$) and adipate ($n = 4$), and rods for suberate ($n = 6$) and sebacate ($n = 8$). The crystals were 80–370 μm in size for the dicarboxylates with an even number of CH_2 groups, except for malonate, while crystals with an odd number of CH_2 groups, glutarate ($n = 3$), pimelate ($n = 5$) and azelate ($n = 7$), were uneven and the size range was below 30 μm.

3.2. X-ray diffraction (XRD) patterns

The XRD patterns of the Mn(II) dicarboxylate hydrates prepared are shown in Fig. 2(a)–(i). These XRD patterns do not show any similarity indicating that they have different crystal structures. The strongest diffraction lines in the dicarboxylates (acids) appear in a narrow 2θ range, 21.2–25.2° (21.4–24.1°), except for 18.3° (29.1°) and 18.5° (23.9°) for oxalate and malonate. The values in parentheses are those of the corresponding dicarboxylic acids. The relationship between the strongest XRD lines and the number of CH_2 groups (n) in the acids and dicarboxylates is shown in Fig. 3. The strongest peaks of dicarboxylates with an even number of CH_2 groups appear in a lower range 21.2–23.6°, while those with an odd number of CH_2 groups are in a higher range, 23.0–25.2°. The values of the strongest XRD lines for the even and odd number of CH_2 groups of the acids and dicarboxylates tend to decrease with increasing n (Fig. 3). In addition, the lines of the acids alternate in character, with higher values for odd numbers and lower values for even numbers of CH_2 groups. However, the lines of the dicarboxylates have lower values with odd numbers and higher values with even numbers of CH_2 groups in the carboxylate unit.

3.3. IR spectra

The IR spectra for Mn(II) dicarboxylate hydrates are shown in Fig. 4, and assignments of the absorption bands are given in Table 2 [8].

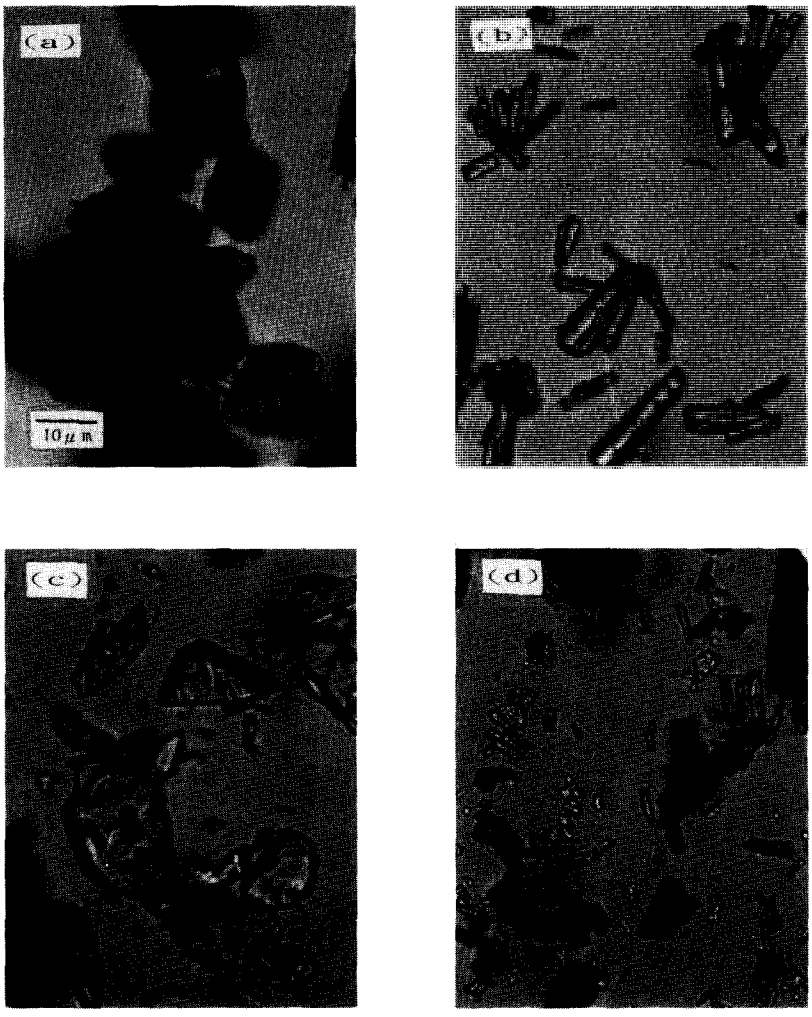

Fig. 1. Optical micrographs of (a) $MnC_2O_4 \cdot 2H_2O$, (b) $MnC_3H_2O_4 \cdot 2H_2O$, (c) $MnC_6H_8O_4 \cdot H_2O$ and (d) $MnC_8H_{12}O_4 \cdot H_2O$.

In the acids and dicarboxylates, the frequencies of most interest with regard to the structures of the dicarboxylates are those of the C–O vibrations. The IR spectra of the dicarboxylic acids show a ν_{asym}(OCO) peak in the vicinity of 1700 cm^{-1} which is indicative of free carboxyl groups [9]. On complex formation, this ν_{asym} (OCO) band is shifted to a lower frequency in all the complexes, showing that complexation is carried out through the carbonyl group [10], and that the O–M bonds in these complexes are essentially electrostatic [11]. Thus it was concluded that the carboxylate group of the acids is coordinated to the Mn(II) ion in the complexes.

Although the $\nu_{asym}(OCO)$ for all the dicarboxylic acids is approximately constant, for the complexes ($n = 6$–8) it tends to decrease with increase in n.

The $\nu_{sym}(OCO)$ band in the complexes was observed between about 1365 cm^{-1} (0–3) and 1410 cm^{-1} (4–8). The increase in the difference ($\Delta\nu$) between $\nu_{asym}(OCO)$ and $\nu_{sym}(OCO)$ has been taken as a measure of the increasing covalency of the M–O bond [12]. Koppikar and Soundararajan [13] observed that the bidentate coordination of the carboxylate group to the metal results in a lowering of both the $\nu(OCO)$ frequencies due to the drainage of the electron density from the carboxylate group to the metal; however, at the same time a decrease in the O–C–O angle results in a decrease in separation ($\Delta\nu$). The IR spectra of the Mn(II) dicarboxylates suggest that the bonding of the carboxylate group to the

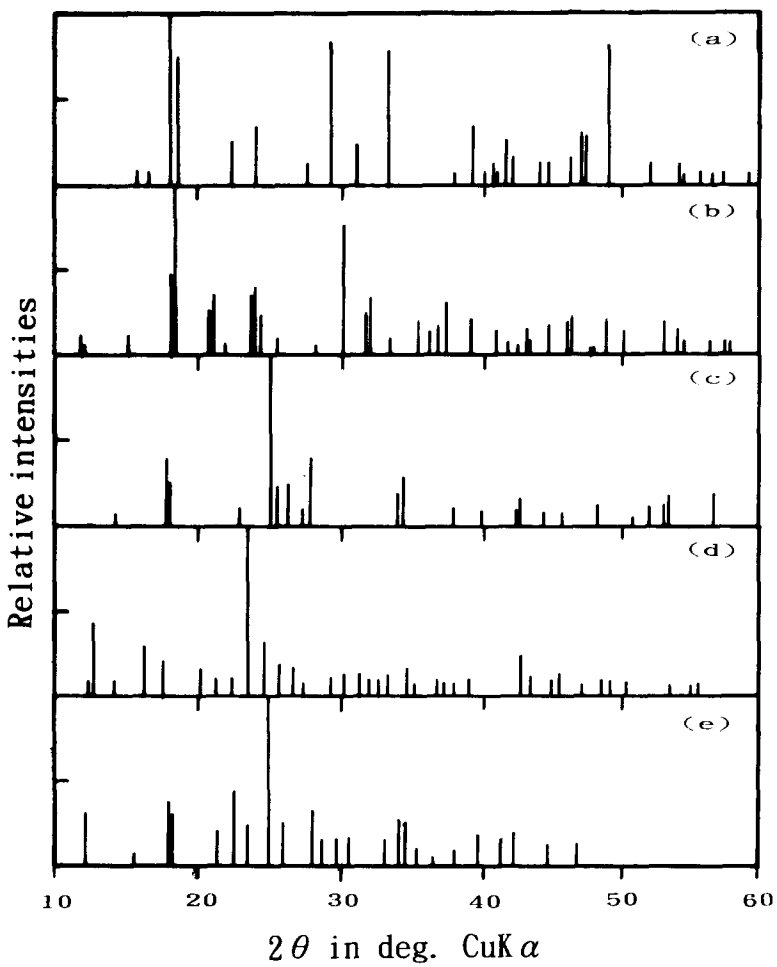

Fig. 2(a).

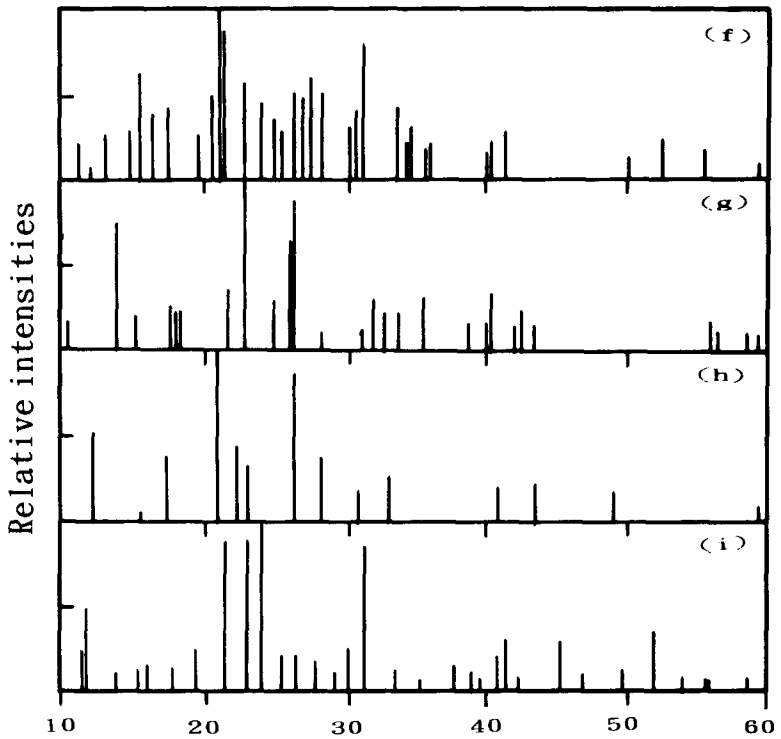

(b)

Fig. 2. X-ray powder diffraction patterns of Mn(II) dicarboxylate hydrates: (a) oxalate; (b) malonate; (c) succinate; (d) glutarate; (e) adipate; (f) pimelate; (g) suberate; (h) azelate; (i) sebacate.

metal is chelating bidentate in these complexes [14]. The relationship between the separation and n for the acids and the dicarboxylates is shown in Fig. 5. The $\Delta\nu$ values for the acids increase with increase in n, while the $\Delta\nu$ values for the dicarboxylates decrease with increase in n. The ν(C=C) absorptions for the dicarboxylates are lower than the corresponding vibration of the free acids showing that no bonding has taken place with the metal ions (Table 2). The complexes of olefins with Ag fluoroborate [15] and the sandwich complexes of cyclopentadiene [16] gave analogous results. An increase in stability of the complex shifts the stretching vibrations of the C=C bond to lower frequencies.

3.4. Dehydration course

The TG–DTA curves of Mn(II) dicarboxylate hydrates are shown in Fig. 6. The TG and DTA curves are denoted by solid and broken lines, respectively. Table 3 lists the n of the dicarboxylates, the number of dehydration stages, the temperature range of successive dehydrations, the temperature for the peak of the DTA curves

Table 2
Infrared absorption data for Mn(II) dicarboxylate hydrates and dicarboxylic acids

Oxalic acid	Oxalate	Malonic acid	Malonate	Succinic acid	Succinate	Glutaric acid	Glutarate	Adipic acid	Adipate	Pimelic acid	Pimelate	Suberic acid	Suberate	Azelaic acid	Azelate	Sebacic acid	Sebacate	Assignment
3700b	3380b		3490b		3400b		3300b		3375b		3400b		3440b		3375b		3475b	$\nu(H_2O)$
			3350b		3150b		3170b		3100b		2980b		3010w		2990vs		3075b	$\nu(H_2O)$
			2900m		2920m		2950m		2916s		2960vs		2970vs		2950vs		2950m	$\nu(H_2O)$
3200b		3300 –		3300 –		3300 –		3300 –		3300 –		3300 –		3300 –		3300 –		ν(OH)
		2500b		2500b		2500b		2500b		2500b		2500b		2500b		2500b		ν(OH)
			1685sb		1690m		1684w											$\delta(H_2O)$
	1654sb		1660w		1650m		1660w				1620w						1595sb	$\delta(H_2O)$
1684s	1620vs	1705m	1566vs	1690s	1570vs	1692s	1576vs	1690s	1574sb	1687s	1570sb	1690s	1560sb	1691s	1540vs	1699s	1535m	$\nu_{asym}(OCO)$
			1454m		1455w		1455m	1462m	1482m	1465m	1460m	1470m	1472w	1470s	1466m	1467m	1462m	$\nu_{sci}(CH_2)$
	1362m		1382vs		1390vs		1403s	1432m	1403s	1422w	1406vs	1422m	1409s	1432m	1400vs	1430m	1400s	$\nu_{sym}(OCO)$
1435m		1439vs		1425s		1424m	1358m	1417m	1348m	1410m	1340vs	1406m	1353vs	1406m	1332m	1405m	1358m	$\nu_{sym}(OCO)$
		1314s		1307vs		1300vs		1296vs		1285s		1313m		1316s		1318m		δ(OH) + ν(CO)
		1178s	1200w	1180s	1222m	1162s	1218w	1197vs	1239m	1197s	1207m	1193s	1198m	1197s	1193w	1190s	1203w	$\nu_{asym}(CC)$
	1196w		1176w		1160w		1128m	1143w	1203m	1140m	1128w	1140m	1102w	1137m	1104w	1140m	1187w	$\nu_{asym}(CC)$
					1106w		1108w		1133vs		1096w		1092w		1092w		1095w	$\nu_{asym}(CC)$
	1010w		1020w		1027m		1073m		1070w		1072w		1032w		1063m		1054m	$\nu_{asym}(CC)$
					1022w		1019m		1041w		1020w		1020w		1018w		1017w	$\nu_{sym}(CC)$
			965vs		965m		934w		950w		950w		945w		946vs		946w	$\nu_{rock}(CH_2)$
			858w		878w				865vs		840w		820m		845m		868m	$\delta_{sci}(OCO)$
	813vs				833w						820w		804w		792m		795vs	$\delta_{sci}(OCO)$
			809vs		800m				798s		770m		790vs		780m		780m	$\delta_{sci}(OCO)$
	738m				755m		762vs		776m				755vs		770m		752w	$\delta_{sci}(OCO)$
			720vs		722w		732m		737s		732m		732w		720vs		720s	$\delta_{wag}(OCO)$
							700m		700m		707m		712m		700w		712m	$\delta_{wag}(OCO)$

Key: b, broad; m, medium; s, strong; v, very; w, weak.

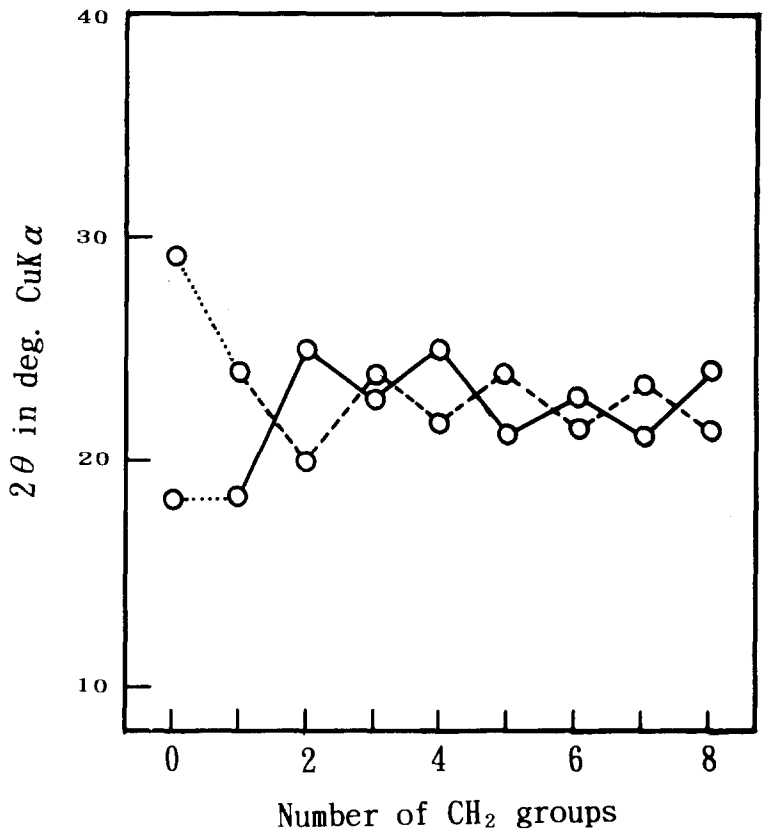

Fig. 3. Relation of the strongest peaks on the X-ray diffraction patterns with the number of CH_2 groups in the Mn(II) dicarboxylate hydrates (solid line) and dicarboxylic acids (broken line).

Table 3
Thermal dehydration data of Mn(II) dicarboxylate hydrates in a flowing Ar atmosphere

Compound	n	Stage	TG temp range/°C	$\Delta(t_i - t_e)$/ °C	DTA peak temp/°C	Weight loss/%		N'
						Obsd.	Calcd.	
$MnC_2O_4 \cdot 2H_2O$	0	1	116–140	24	134	20.09	20.13	2
$MnC_3H_2O_4 \cdot 2H_2O$	1	1	128–210	82	184	18.52	18.67	2
$MnC_4H_4O_4 \cdot 4H_2O$	2	1	88–136	48	111	28.81	29.64	4
$MnC_5H_6O_4 \cdot 4H_2O$	3	1	67–120	53	106	27.24	28.03	4
$MnC_6H_8O_4 \cdot H_2O$	4	2	151–240	89	191	7.85	8.30	1
$MnC_7H_{10}O_4 \cdot H_2O$	5	2	81–119	38	108	7.53	7.80	1
$MnC_8H_{12}O_4 \cdot H_2O$	6	2	120–192	72	162	7.28	7.35	1
$MnC_9H_{14}O_4 \cdot H_2O$	7	2	56–148	92	81	6.50	6.95	1
$MnC_{10}H_{16}O_4 \cdot H_2O$	8	2	65–146	81	98	6.43	6.59	1

Key: N', water molecules lost by dehydration; t_i and t_e, initial and end temperatures for weight loss.

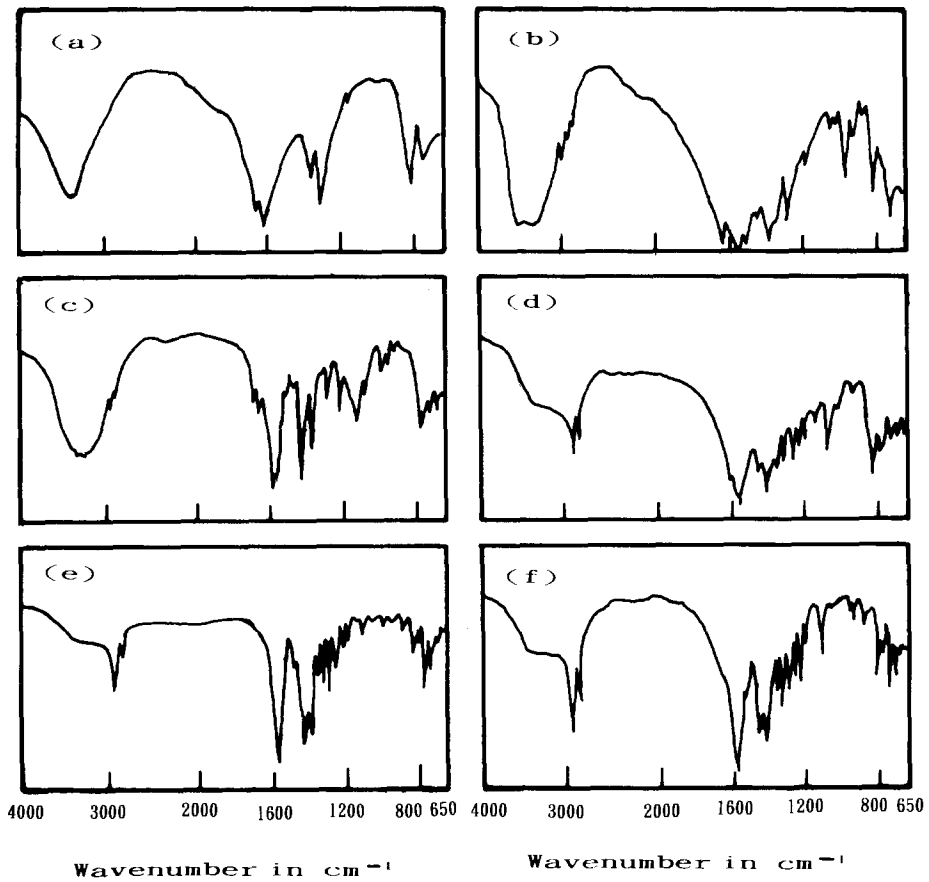

Fig. 4. Infrared spectra of Mn(II) dicarboxylate hydrates: (a) oxalate; (b) malonate; (c) glutarate; (d) adipate; (e) suberate; (f) sebacate.

(T_D), the weight loss after complete dehydration and the number of water molecules lost on dehydration (N'). The dehydration processes in Ar, CO_2 and air for the Mn(II) oxalate to glutarate hydrates ($n = 0, 1-3$) show a single step, and the Mn(II) adipate to sebacate hydrates ($n = 4-8$) show two steps. The dehydration behaviour of the dicarboxylates was little affected by the atmosphere, i.e. Ar, CO_2 and air. The observed weight losses for these processes agreed favourably with the calculated water of hydration. The smoothness of the TG and DTA curves and the agreement between the calculated and observed values of weight loss for the dicarboxylates ($n = 0, 1-8$) suggest that dehydration takes place in similar ways. The endothermic peaks on the DTA curves correlate with loss of water from the crystals. The TG–DTA curves of the dicarboxylates (1–8) in flowing Ar, CO_2 and air atmospheres indicate slow dehydration with a broad endothermic peak, while the Mn(II) oxalate dihydrate dehydrated rapidly with a somewhat sharp endothermic peak at 134°C. It is possible to suggest that the water of crystallization

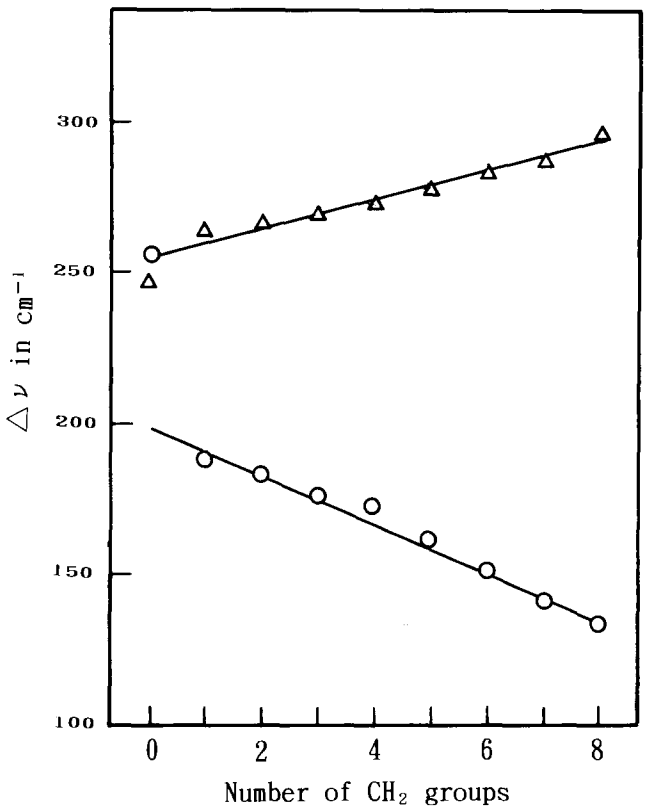

Fig. 5. Relation between separation Δν and the number of CH_2 groups in Mn(II) dicarboxylate hydrates (○) and dicarboxylic acids (△).

molecules are bonded in two different ways: the water lost at lower temperatures is outer sphere, and the water lost at higher temperatures is coordination water which is strongly bonded with an Mn ion. The initial weight loss temperature (T_i), or the temperature from which the TG curve begins to drop, may be taken as a measure of the relative strengths of the Mn^{m+}–OH_2 bonds. The relationship between T_i and n of the dicarboxylates is given in Fig. 7.

These plots have a similar tendency to those for the strongest peaks on the XRD diagrams and the n of the dicarboxylates described above which were found to change periodically with increasing n.

Heating all the salts at 190°C in the various atmospheres causes a slight decrease in the intensities of the IR absorption bands and XRD signals; at this stage no structural alternation is shown by XRD. From dehydration of the Mn(II) dicarboxylate hydrates, the XRD patterns showed that the crystallinity was somewhat decreased and microscopic observation showed that the particle sizes of the hydrates were subdivided.

Table 4
Activation energy E_a (in kcal mol^{-1}) [a] and frequency factor A (in s^{-1}) for initial and main reaction of Mn(II) dicarboxylate hydrates in various atmospheres

Compound		Stage	Ar						CO_2						Air					
			Initial		Main			Model	Initial		Main			Model	Initial		Main			Model
			E_a	A	E_a	A	γ		E_a	A	E_a	A	γ		E_a	A	E_a	A	γ	
Oxalate	($n=0$, $X=2$)	I	10.1	1.07	67.0	1.37×10^{16}	0.9987	[D3]	11.5	1.15	57.9	7.24×10^{15}	0.9990	[D3]	11.7	1.06	79.2	7.12×10^{20}	0.9992	[D3]
Malonate	($n=1$, $X=2$)	I	11.2	2.90	32.6	1.87×10^{9}	0.9981	[D3]	11.2	3.24	31.6	8.26×10^{8}	0.9978	[D3]	11.1	3.05	33.3	2.63×10^{9}	0.9987	[D3]
Succinate	($n=2$, $X=4$)	I	9.34	2.65	35.4	1.19×10^{11}	0.9990	[D3]	9.90	2.27	40.1	1.79×10^{12}	0.9986	[D3]	10.3	1.83	47.8	1.78×10^{14}	0.9983	[D3]
Glutarate	($n=3$, $X=4$)	I	9.56	2.30	29.3	3.03×10^{9}	0.9978	[D3]	9.65	1.95	32.0	2.89×10^{10}	0.9983	[D3]	10.1	1.61	27.7	3.40×10^{9}	09986	[D3]
Adipate	($n=4$, $X=1$)	I	12.3	1.82	45.3	1.31×10^{11}	0.9993	[D3]	11.7	2.70	56.4	1.90×10^{13}	0.9987	[D3]	13.1	1.61	52.4	2.24×10^{12}	0.9988	[D3]
Pimelate	($n=5$, $X=1$)	I	9.77	1.99	29.0	3.51×10^{9}	0.9994	[D3]	10.8	1.07	29.5	4.32×10^{9}	0.9984	[D3]	10.2	1.05	18.4	8.55×10^{6}	0.9990	[D3]
		II	11.5	1.67	47.8	1.58×10^{12}	0.9988	[D3]	12.3	1.03	62.8	1.22×10^{15}	0.9991	[D3]	10.3	1.43	35.9	5.92×10^{10}	0.9978	[D3]
Suberate	($n=6$, $X=1$)	I	13.6	1.42	32.6	6.81×10^{10}	0.9985	[R2]	14.1	3.40	26.8	3.85×10^{8}	0.9988	[R2]	17.1	1.11	33.1	7.36×10^{9}	0.9985	[R2]
		II	–	–	–	–			–	–	–	–			–	–	–	–		
Azelate	($n=7$, $X=1$)	I	–	–	21.7	9.84×10^{7}	0.9991	[D3]	–	–	41.0	3.57×10^{13}	0.9992	[D3]	–		18.5	1.27×10^{7}	0.9989	[D3]
		II	10.5	1.67	38.1	6.63×10^{10}	0.9986	[D3]	10.9	2.09	19.6	6.92×10^{6}	0.9983	[D3]	10.5	1.26	39.4	7.84×10^{10}	0.9985	[D3]
Sebacate	($n=8$, $X=1$)	I	8.31	2.41	32.0	5.53×10^{10}	0.9979	[D3]	10.2	1.05	29.6	1.29×10^{10}	0.9987	[D3]	10.6	1.27	29.7	1.32×10^{10}	0.9986	[D3]
		II	9.48	2.83	26.3	2.98×10^{8}	0.9983	[D3]	10.7	1.17	23.3	5.43×10^{7}	0.9985	[D3]	10.6	1.12	34.9	3.31×10^{10}	0.9979	[D3]

Key: D3, $F(\alpha) = [1-(1-\alpha)^{1/3}]^2$; R2, $F(\alpha) = 1-(1-\alpha)^{1/2}$; γ, correlation coefficient. [a] 1 kcal is 4.18 J.

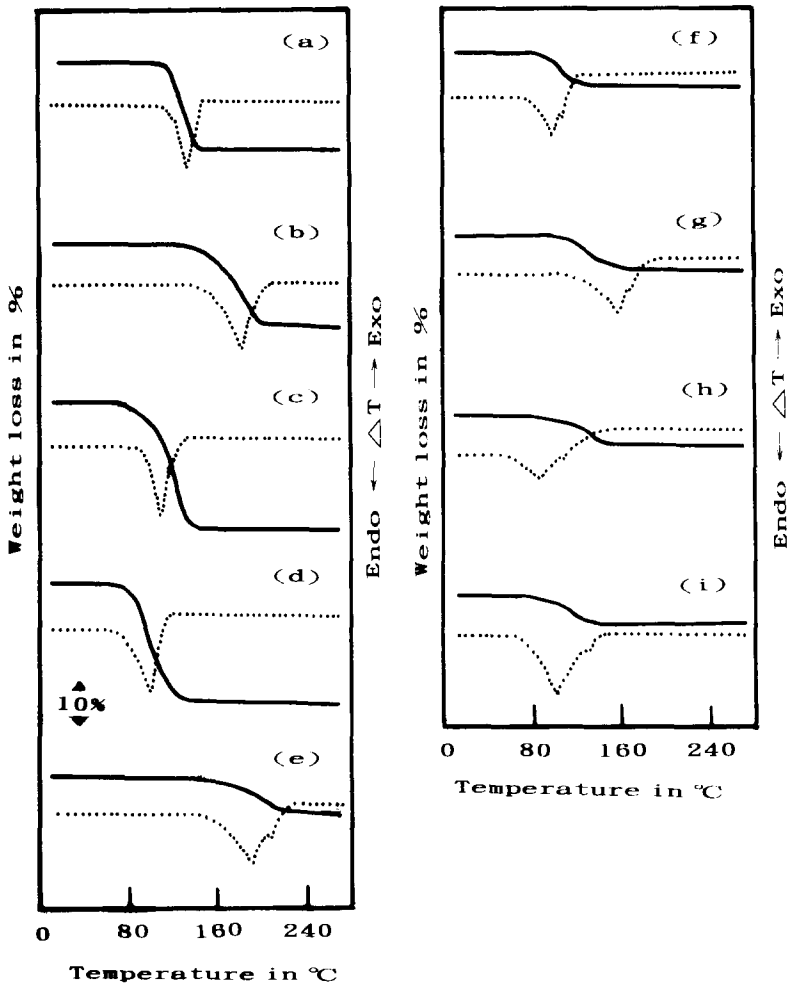

Fig. 6. TG–DTA curves for the thermal dehydration of Mn(II) dicarboxylate hydrates in a flowing Ar atmosphere: (a) $MnC_2O_4 \cdot 2H_2O$; (b) $MnC_3H_2O_4 \cdot 2H_2O$; (c) $MnC_4H_4O_4 \cdot 4H_2O$; (d) $MnC_5H_6O_4 \cdot 4H_2O$; (e) $MnC_6H_8O_4 \cdot H_2O$; (f) $MnC_7H_{10}O_4 \cdot H_2O$; (g) $MnC_8H_{12}O_4 \cdot H_2O$; (h) $MnC_9H_{14}O_4 \cdot H_2O$; (i) $MnC_{10}H_{16}O_4 \cdot H_2O$. TG, solid line; DTA, dotted line.

The diffusion mechanism of the dehydration reaction of Mn(II) dicarboxylate hydrates assumes that the effective area of the reaction interface does not change with the degree of reaction (α), and the rate of evolution of water from the hydrates can be controlled by the rate of three-dimensional diffusion (D3 function) of the appropriate constituent to the active surface. Therefore, it is suggested that the water is loosely accommodated within the channels of the lattice from which escape occurs with minor structural reorganization.

The comparison of fit to the various kinetic equations (those commonly used in kinetics analyses for solid state reaction, namely D1–D4, F1–F3, R1–R3, A2–A3)

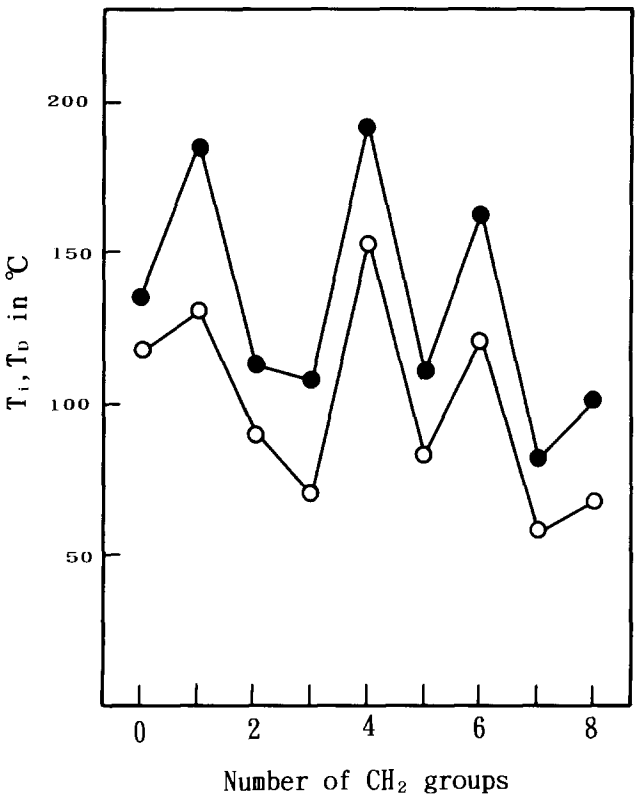

Fig. 7. Relation between T_i, T_D and the number of CH_2 groups of Mn(II) dicarboxylate hydrates in flowing Ar atmosphere: ○, initial dehydration temperature (T_i); ●, DTA peak temperature (T_D).

for the initial and main reactions, see Table 4, shows that the best fit of data of the main dehydration for most of the Mn(II) dicarboxlate hydrates is obtained with the three-dimensional diffusion (D3 function) model. The activation energy E_a and frequency factor A were in good agreement for the kinetic analysis which divided the initial and main reaction on TG curves of the decomposition of dicarboxylic acids as defined in Ref. [17]. The two-dimensional phase boundary reaction R2 was also fitted, but only for Mn(II) suberate. However, when mechanisms other than D3 were selected a somewhat poor correlation coefficient was obtained for the R3 function. The kinetic parameters were calculated by employing a computational method. The computer flow diagram for calculation of activation energy and frequency factor were calculated by the least-squares method of Ref. [17]. The relation between activation energy E_a for the initial and main dehydration [17] versus the number of CH_2 groups for the salts is shown in Fig. 8. The plots of Figs. 7 and 8 follow zig-zag lines which is presumed to reflect the zig-zag structure of the dicarboxylic acids.

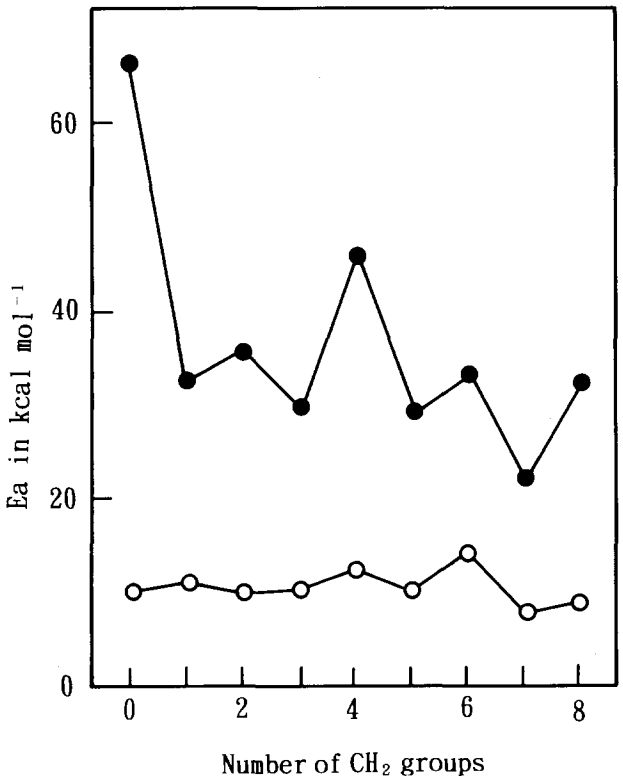

Fig. 8. Relation between activation energy E_a and number of CH_2 groups n in the dehydration of Mn(II) dicarboxylate hydrates in flowing Ar atmosphere: ○ and ● are initial and main reactions.

Acknowledgment

The author thanks Dr K. Muraishi, Yamagata Women's Junior College, for many helpful discussions and suggestions during this work.

References

[1] Beilstein Handbuch der Organischen Chemie, Vols. 2–3, Springer, Berlin, 1976, Syst. Nr. 171–179, s. 1877–2202.
Gmelin Handbuch der Anorganischen Chemie, Mn, Koordinations-Verbindungen 2, Springer, Berlin, 1980 Syst. Nr. 56, s. 125–141.
[2] W.E. Brown, D. Dollimore and A.K. Galwey, in C.H. Banford and C.F.H. Tipper (Eds.), Comprehensive Chemical Kinetics, Vol. 22, Reaction in the Solid State, Elsevier, Amsterdam, 1980, p. 208.
[3] J.R. Allen, B.R. Carson, D.L. Gerrard and S. Hoey, Thermochim. Acta, 158 (1990) 91.
[4] J.R. Allen, J.G. Bonner, H.J. Bowley, D.L. Gerrard and S. Hoey, Thermochim. Acta, 141 (1989) 227.

[5] N.J. Carr and A.K. Galwey, Proc. R. Soc. London Ser. A, 404 (1986) 101.
[6] Y. Suzuki, K. Muraishi and K. Matsuki, Thermochim. Acta, 211 (1992) 171.
[7] J.H. Sharp, G.W. Brindley and B.N.N. Achar, J. Am. Ceram. Soc., 49 (1966) 379.
D. Dollimore, T.A. Evans, Y.F. Lee and F.W. Wilburn, Thermochim. Acta, 188 (1991) 77.
A.R. Salvador and E.G. Calvo, Thermochim. Acta, 203 (1992) 67.
[8] K. Muraishi and K. Nagase, Thermochim. Acta, 159 (1990) 225.
[9] N.B. Colthup, J. Opt. Soc. Am., 40 (1950) 397.
[10] D.H. Bush and J.G. Bailar, Jr., J. Am. Chem. Soc., 75 (1953) 4574.
S. Kirrschner, J. Am. Chem. Soc., 78 (1956) 2372.
P.V. Khadikar and N.S. Sapre, Thermochim. Acta, 128 (1988) 55.
[11] D.K. Koppikar and S. Soundararajan, Curr. Sci., 45 (1976) 3.
[12] K. Nakamoto, Y. Morimoto and A.F. Martel, J. Am. Chem. Soc., 83 (1961) 4524.
P.V. Khadikar, S.M. Ali and B. Heda, J. Therm. Anal., 30 (1985) 305.
[13] D.K. Koppikar and S. Soundararajan, Monatsh. Chem., 107 (1976) 105.
[14] G.B. Deacon and R.J. Phillips, Coord. Chem. Rev., 33 (1980) 227.
[15] H.W. Quinn, J.S. McIntyre and D.J. Peterson, Can. J. Chem., 43 (1965) 2896.
[16] E.R. Lindguist and E.D. Nelson, Spectrochim. Acta, 10 (1958) 307.
[17] K. Muraishi, Y. Suzuki and A. Kikuchi, Thermochim. Acta, 239 (1994) 51.